



Characterization and Electrochemical Performance of Composite BSCF Cathode for Intermediate-temperature Solid Oxide Fuel Cell

Yu-Mi Kim^a, Pattaraporn Kim-Lohsoontorn^{b,c} and Joongmyeon Bae^{a,c,†}

^aDepartment of Mechanical Engineering, Korea Advanced Institute of Science and Technology (KAIST), Daejeon, 305-701, Republic of Korea

^bDepartment of Chemical Engineering, Mahidol University, Nakorn Pathom, 73170, Thailand

^cKI for Eco-Energy, Korea Advanced Institute of Science and Technology (KAIST), Daejeon 305-701, Republic of Korea

ABSTRACT :

The composite barium strontium cobalt ferrite (BSCF) cathodes were investigated in the intermediate temperature range of solid oxide fuel cells (SOFCs). The characteristics and electrochemical performances of composited BSCF/samarium doped ceria (SDC); BSCF/gadolinium doped ceria (GDC); and BSCF/SDC/GDC were compared to single BSCF cathode. The BSCF used in this study were synthesized using glycine nitrate process and mechanically mixing was used to fabricate a composite cathode. Using a composite form, the thermal expansion coefficient (TEC) could be reduced and BSCF/SDC/GDC exhibited the lowest TEC value at $18.95 \times 10^{-6} \text{ K}^{-1}$. The electrochemical performance from half cells and single cells exhibited nearly the same trend. All the composite cathodes gave higher electrochemical performance than the single BSCF cathode (0.22 Wcm^{-2}); however, when two kinds of electrolyte were used (BSCF/SDC/GDC, 0.36 Wcm^{-2}), the electrochemical performance was lower than when the BSCF/SDC (0.45 Wcm^{-2}) or BSCF/GDC (0.45 Wcm^{-2}) was applied as cathode (650°C , $97\% \text{H}_2/3\% \text{H}_2\text{O}$ to the anode and ambient air to the cathode).

Keywords : Composite electrode, Cathode, Anode-supported solid oxide fuel cell, Barium strontium cobalt ferrite, Gadolinium doped ceria, Samarium doped ceria

Received January 31, 2011 : Accepted February 14, 2011

1. Introduction

Solid oxide fuel cells (SOFCs) have the merits of low pollutant emission, high efficiency of the energy conversion and flexibility to multiple fuel choices. Contrary to high-temperature SOFCs, which are commonly operated above 800°C , the intermediate temperature SOFCs (IT-SOFC) have been investigated and gain much interest due to the advantages of manufacturing cost reduction and variety of material choices.^{1,2)} In general, lowering

the operating temperature leads to performance decay due to increasing internal resistance of the cells, and most of the increasing resistance are well known to be generated from cathode parts.²⁾ Therefore, many researchers have been focusing on the development of cathode materials which exhibit high electrocatalytic activities at intermediate temperature ranges.^{3,4,5,6)} Under these circumstances, various ways have been used for improving the electrochemical performances at intermediate temperatures such as synthesis of new composition/structured materials,³⁾ impregnation of noble metal⁴⁾ and development of composite electrode.^{5,6)} Among the various approaches, composite cathode which

[†]Corresponding author. Tel.: +82-42-350-3045

E-mail address: jmbae@kaist.ac.kr

comprises of mechanically mixed cathode and electrolyte constituents is known as one of the simplest ways which potentially provides an expected outcome. Using the composite cathode can reduce the thermal expansion difference between cathode and electrolyte layer, improving the chemical compatibility between cathode and electrolyte layer and thereby improving long term stability of SOFCs.

The perovskite compounds with ABO_3 structure are generally used as cathode.^{7,8)} In the case of widely used strontium-doped lanthanum manganites ($La_{1-x}Sr_xMnO_{3-\delta}$, LSM), most of oxygen reduction reaction occurs on the three phase boundary of electrode/electrolyte/gas phase due to the pure electronic conducting behavior of LSM. Therefore, mixing with yttria stabilized zirconia (YSZ) electrolyte, which has high ionic conductivity, can extend the reaction sites to a whole cathode structure. This helps activate the oxygen reduction reaction and finally improve the electrochemical performance. Although cathode materials exhibit mixed ionic and electronic conductivity such as $La_{1-x}Sr_xCo_yFe_{1-y}O_{3-\delta}$ (LSCF)⁹⁾ or $Sm_xSr_{1-x}CoO_{3-\delta}$ (SSC),¹⁰⁾ composite electrodes of LSCF or SSC with electrolyte materials are also generally made to improve adhesion between cathode and electrolyte.

The barium strontium cobalt ferrites ($Ba_{1-x}Sr_xCo_{1-y}Fe_yO_{3-\delta}$, BSCF) using in this study are a promising candidate for SOFC cathode,^{11,12)} and also have been investigated as composite cathodes by mixing with electrolyte materials. Gadolinium doped ceria (GDC) and samarium doped ceria (SDC) have been considered as suitable electrolyte materials for IT-SOFC because of its high ionic conductivity at intermediate temperature range. Kao *et al.*¹³⁾ reported that the cell with a BSCF/GDC composite electrode synthesized by GNP method exhibited the maximum power density of 0.19 W cm^{-2} at $750^\circ\text{C}\cdot\text{K}$. Wang *et al.*¹⁴⁾ showed that the BSCF/SDC composite cathode by mechanical milling provided significantly improved performance of 0.38 W cm^{-2} at 500°C . The remarkable performance improvement by using composite electrode such as LSM/YSZ or LSCF/GDC has also been reported previously.^{9,10,13,14)} Improving cathode performance by using a composite form should be therefore further studied. Moreover, most of researchers synthesized the composite electrode from mixing the cathode with single electrolyte powder. Therefore, it is interesting to investigate the effect of two kinds of electrolytes used in composite cathode.

In this study, BSCF as a raw cathode; and, GDC and SDC as a raw electrolyte were used in order to investigate the electrochemical performance and characteristics of

composite cathode. Single BSCF electrode and three kinds of composite electrodes: BSCF/SDC, BSCF/GDC and BSCF/SDC/GDC; were prepared for the experiments. The positive and negative effect of composting two electrolytes with BSCF cathode was found in this study. All composite electrodes were synthesized via mechanical mixing method. The microstructure of electrode and thermal expansion behaviors were characterized by scanning electron microscopy (SEM) and thermo-gravimetric analysis (TGA), respectively. The phase compositions of the electrode were analyzed by X-ray diffraction (XRD), and the electrochemical performance and ac-impedance spectroscopy of the cells having composite BSCF cathode were measured as a function of temperature.

2. Experimental

2.1. Preparation of cathode powders

BSCF powders were prepared by the glycine nitrate process (GNP).¹⁴⁾ Appropriate amounts of $Ba(NO_3)_2$, $Sr(NO_3)_2$, $Co(NO_3)_2\cdot 6H_2O$ and $Fe(NO_3)_3\cdot 9H_2O$ powders (Alfa Aesar, USA) were initially dissolved with glycine ($C_2H_5NO_2$) in deionized water. The solution was then heated until it ignited. The ignited powder was calcined in air at 1000°C for 8 h. The calcined powders were collected by using 100 and $38 \mu\text{m}$ sieve. In order to make the powder smaller, the wet ball-milling with powder, acetone and zirconia ball was conducted for 24h. After removing the acetone by drying at 80°C for 12 h, the BSCF powder was dispersed in combinations of 20 wt.% α -terpineol with 80 wt.% cellulose to obtain the cathode ink.

In order to make composite cathode powder, the commercial GDC (ANAN KASEI, Japan) and SDC (FCM, USA) powder were used as raw material. Synthesized BSCF and commercial electrolyte powder were then mixed with the weight ratio of 7 : 3. For example, the composite cathodes were prepared as follows:

BSCF : GDC = 7 : 3,

BSCF : SDC = 7 : 3,

BSCF : GDC : SDC = 7 : 1.5 : 1.5.

The prepared powders were ball-milled with acetone for 24 h in order to create uniformly mixed powders. After this process, the resulting solutions were heated at 80°C for 12 h to dry out the acetone. The composite cathode ink for composite powder was then produced using the same way as the BSCF ink.

2.2. Fabrication of the cell

For half cell test, a GDC powder was uniaxially pressed

(10 MPa for 60 s), followed by sintering at 1500°C in air for 4 h - giving a dense pellet (~95% calculated density) with a diameter of ~26.0 mm and thickness of ~1.2 mm. After that, the cathode layers were screen-printed on both sides of the GDC pellet, and heated at 200 °C for 12 h in order to dry out the cathode layer. Sintering was carried out at 1000°C for 2 h to obtain sintered cathode layers with a circular area of 0.785 cm² and a thickness of ~16 μm.

For single cell test, in order to fabricate the anode-supported cell, NiO powder (J.T. Baker, USA) and 8YSZ (Tosho, Japan) powder were mixed in a weight ratio of 6 : 4 and ball-milled for 24 h using ethanol as media. 12 wt% of starch was added as a pore former to create sufficient porosity in the anode. The mixed powder was pressed into a pellet, followed by sintering at 1200°C for 2 h - giving a pellet with a diameter of ~26.0 mm and thickness of ~1.1 mm. The YSZ slurry was blended with compositions of 15 wt.% of binder (butvar B-98), 2 wt.% of dispersant (polyvinylpyrrolidone), 10 wt.% of plasticizer (polyethyleneglycol), and balanced weights of the YSZ powder. The YSZ slurry was ball-milled for 36 h. The dip coating technique was used to deposit of YSZ electrolyte layer, followed by sintering the YSZ dipped anode at 1500°C for 4 h. The GDC buffer layer was deposited on the YSZ electrolyte in order to block the chemical reactions between YSZ electrolyte and cathode. The cobalt-based cathodes, including BSCF, are not compatible with YSZ electrolyte, producing interfacial insulating layers during high temperature exposure, which leads to a degradation in cell performance.^{15,16} It is known that CeO₂ is compatible with YSZ.¹⁷ Therefore, this ceria-based material was used as a buffer layer between the cathode and electrolyte. The GDC buffer layer was sintered at 1300°C for 4 h, and the area of the buffer layer is about 1.45 cm². After that the cathode was screen-printed on the buffered pellet and was sintered at 1000°C for 2 h - giving a cathode area of 0.785 cm².

2.3. Characterization of electrode and electrochemical measurement

The XRD patterns of the BSCF and composite powders were obtained from XRD (Rigaku D/MAX III C, Japan) using Cu K α radiation ($\lambda = 1.5428 \text{ \AA}$) at 40 kV and 40 mA. The XRD data were collected at 0.01° with a counting time of 1 s per step in the 2 θ range from 20° to 80°. The SEM images of the cell were taken with 15 kV (HITACHI FE-SEM S-4300, Japan). In order to measure the thermal expansion behavior, the synthesized

powder was pelletized with a rectangular shape of 15 mm \times 5 mm, and sintered at 1000°C for 2 h. The thermal expansion behaviors were measured from dilatometer (NETZSCH, Germany) with the temperature range of 25~900°C.

2.4. Electrochemical performance measurement

The I-V-P characteristics of single cell were measured using linear sweep current techniques. The impedance measurement of half cells was performed at open circuit voltage (OCV) under potentiostatic mode using a sinusoidal signal amplitude of 20 mV_{rms}, over the frequency range of 10⁶ Hz to 10⁻² Hz. The impedance spectroscopy was collected using Solartron, SI 1287 ECI, fitted with a frequency response analyzer (Solartron, SI 1255 FRA, USA).

Electrical connection was made to the cell via platinum wires and paste which were put into compression. For half cell measurements, the cell holder was then placed inside a quartz tube, with gas inlet and outlet points, permitting control over the gaseous environment to which the cell was exposed. A tube furnace was used to control the temperature of the test rig. For a single cell measurement, the cell ridge was sealed using sealant (Ultra-temp 516, Aremco, USA) to isolate the gas environments of the two electrodes. The test system allows gas composition H₂/N₂ to be introduced to the anode with the total flow rate of 50 sccm and the ambient air was fed to the cathode with 100 sccm. The H₂/N₂ line passes through the humidifier in order to humidify the flowing gas with water at the required level (3 mol% humidified H₂). Detailed test configurations were explained in previous study.¹⁸⁾

3. Results and Discussion

3.1. Characterization of composite electrode

Fig. 1 showed the XRD patterns obtained from BSCF, GDC, SDC and three composite cathode powders (BSCF/SDC, BSCF/GDC, BSCF/GDC/SDC). The electrolytes (SDC and GDC) and BSCF powders exhibited the XRD patterns of fluorite and perovskite structure, respectively. It was observed that the peaks for impurities were not detected from all electrolytes and BSCF powders under the detection limit. Moreover, from the XRD patterns of the composite cathode powders, the peaks for BSCF and each electrolyte could be individually divided. As shown in Fig. 1, there are no significant impurities observed from the XRD pattern because the composite powder was just mechanically mixed, not sintered for cathode fabrication at high temperature. According to the work of Wang *et al.*,¹⁴⁾

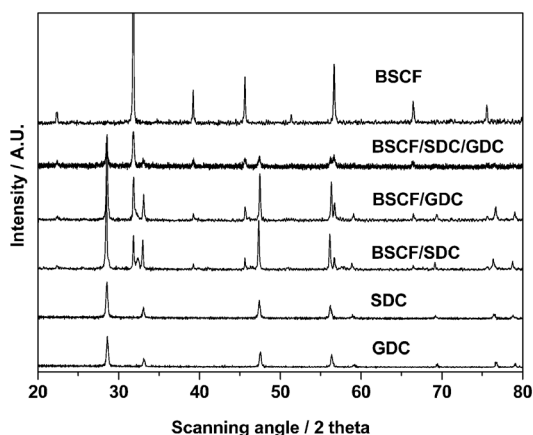


Fig. 1. The XRD patterns obtained from single BSCF, and three kinds of composite BSCF cathodes (BSCF/SDC, BSCF/GDC, and BSCF/SDC/GDC).

in the case of BSCF/SDC composite cathode which was sintered at 1000°C for 2 h, peaks for new perovskite phase were observed near the right side of the main BSCF peaks. Furthermore, a weak peak for (Ba,Sr)CeO₃ was also detected from the XRD patterns of BSCF/SDC composite electrode. When the composite electrodes are sintered at 1100°C, it is reported that the BSCF phase completely disappeared, while the intensity of new perovskite phase was

obviously strengthened.¹⁴⁾ In the present study, the composite electrodes were sintered at 1000°C for 2 h, therefore the effect of impurities on the electrochemical performance from high-temperature sintering process could be negligible.

The SEM images from various composite electrodes are shown in Fig. 2. Fig. 2(a), (b) and (c) are surface morphologies obtained from BSCF/SDC, BSCF/GDC and BSCF/SDC/GDC, respectively. All samples were sintered at 1000°C for 2 h before SEM images were taken. From the images, it can be observed that all electrodes had a porous microstructure, and the electrolyte powders with small size were uniformly distributed on the cathode. Moreover, the BSCF/SDC and BSCF/GDC composite electrodes shown in Fig. 2(a) and (b) had the main particle size of 1~5 μm, however, it was observed in Fig. 2(c) that the BSCF/SDC/GDC composite electrode contained larger particle size than that of the other electrodes. Fig. 2(d) shows the enlarged SEM images of the BSCF/SDC cathodes in order to observe the cathode and electrolyte particles. It is observed that the electrolyte particles are well adhered to the cathode surface. When the GDC and SDC were mixed with cathode powders followed by sintering at 1000°C for 2 h, the improved sintering phenomena were observed. The reason for this improved sintering behavior is unclear but it is likely due to the effect of mixed GDC/SDC electrolyte powders. These differences

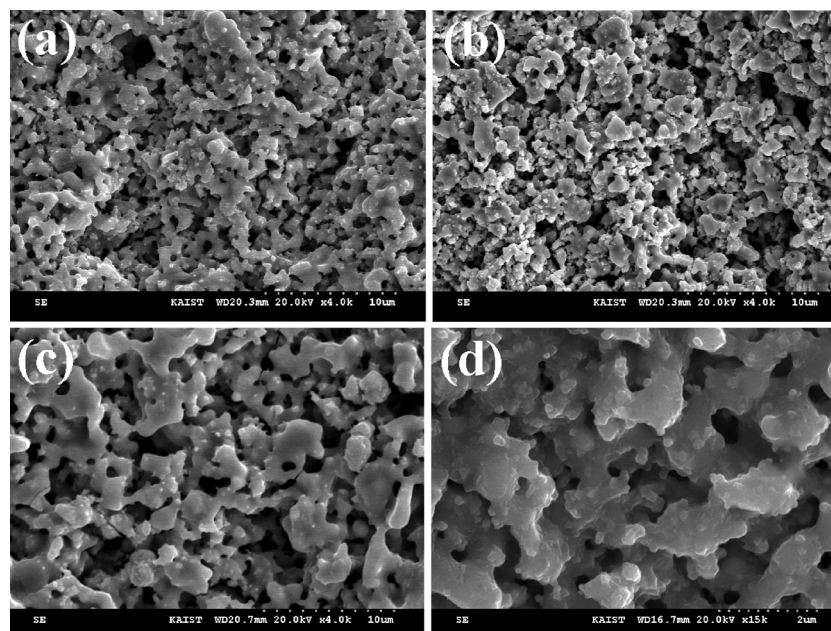


Fig. 2. The SEM images of the (a) BSCF/SDC, (b) BSCF/GDC, (c) BSCF/SDC/GDC composite cathodes surface, and (d) enlarged BSCF/SDC composite cathodes after sintering at 1000°C for 2 h.

in sintered particle sizes have not been reported elsewhere, and it is interesting to investigate further about the causes for this sintering behaviors. The SEM image from cross section of the half cell is introduced in Fig. 3, which shows the BSCF/SDC/GDC composite cathode layer on GDC electrolyte after sintering at 1000°C for 2 h. The GDC electrolyte layer was fairly dense, and the thickness of cathode was determined to be about 20~25 μm . Also, from the SEM images, it can be confirmed that the cathode layer was formed as a porous structure.

Fig. 4 represents thermal expansion behaviors of single and composite electrodes as a function of temperature ranging from 30 to 900°C. The similar behaviors from all electrodes were observed; however, the composite cathode showed more linear behaviors than the single BSCF

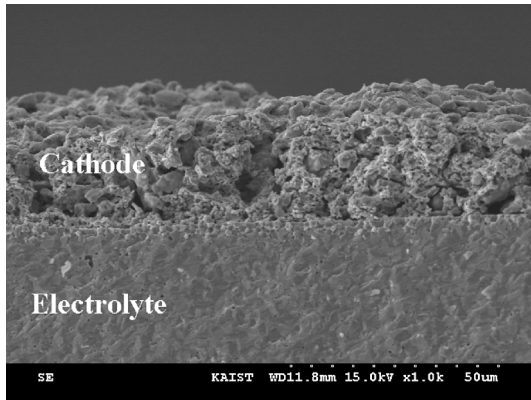


Fig. 3. Cross-sectional SEM image of the BSCF/SDC/GDC composite cathode on GDC electrolyte after sintering at 1000°C for 2 h.

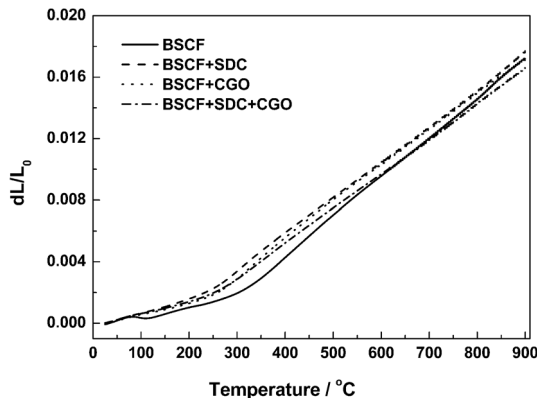


Fig. 4. Thermal expansion behaviors of single BSCF, BSCF/SDC, BSCF/GDC and BSCF/SDC/GDC electrodes measured from room temperature to 900°C.

Table 1. Calculated TEC values based on the thermal expansion behaviors of BSCF/SDC, BSCF/GDC, BSCF/SDC/GDC composite cathodes and single BSCF cathode as shown in Fig. 4

Electrode	TEC ($\times 10^{-6} \text{K}^{-1}$)	Error
BSCF	19.77	5.2×10^{-9}
BSCF/SDC	19.23	4.3×10^{-9}
BSCF/GDC	19.32	4.0×10^{-9}
BSCF/SDC/GDC	18.95	7.3×10^{-9}

electrode. Table 1 shows the calculated thermal expansion coefficients (TECs) obtained from TEC behaviors of single and composite BSCF electrodes. Thermal behavior was measured from room temperature to 900°C, while the TEC values were calculated by using the data from 100 to 900°C. In Table 1, it is observed that the BSCF electrode had TEC value of $19.77 \times 10^{-6} \text{K}^{-1}$, closely corresponding to the work of McIntosh *et al.*¹⁹⁾ The composite electrode BSCF/SDC and BSCF/GDC showed slightly lower value of $19.23 \times 10^{-6} \text{K}^{-1}$ and $19.32 \times 10^{-6} \text{K}^{-1}$, respectively than the single BSCF electrode. The lowest TEC values of $18.95 \times 10^{-6} \text{K}^{-1}$ among the electrodes was obtained from the BSCF/SDC/GDC electrode. From this result, the TEC values of composite electrodes were lower than single electrode and composite of BSCF with two kinds of electrolyte could lower the TEC value. It should be noted that the mixing ratio of electrolyte and cathode powder was fixed as 30 : 70 wt.%. From this fact, it can be concluded that mixing two electrolytes with the cathode powder have positive effects on decreasing TEC. All calculated TEC values have the error ranges of $\pm 4.0 \sim 7.3 \times 10^{-9}$.

3.2. Electrochemical measurement of composite electrode

The impedance behaviors as a function of temperature were measured from both single and three kinds of composite electrodes as shown in Fig. 5. The 4-probes method was used in this measurement while the temperature for the half cell test was varied from 500 to 850°C. In the case of BSCF/SDC/GDC composite electrode, the higher area specific resistance (ASR) than other composite electrodes (BSCF/SDC and BSCF/GDC) were observed at intermediate temperature over 600°C while rather similar ASR values to other composite electrodes were observed below 600°C. The BSCF/SDC and BSCF/GDC composite electrodes showed uniformly higher performance than that of single electrode. The ASR values of composite electrodes were nearly two times lower than that of the BSCF electrode for the whole temperature ranges. Among

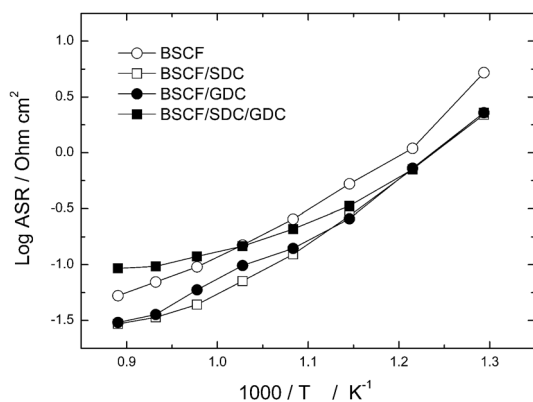


Fig. 5. The electrochemical performance measured from the half cells having BSCF, BSCF/SDC, BSCF/GDC and BSCF/SDC/GDC cathodes as a function of temperature.

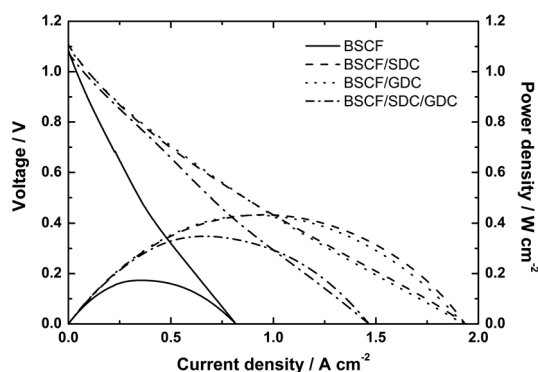


Fig. 6. I-V-P characteristics of the single cells having BSCF, BSCF/SDC, BSCF/GDC, BSCF/SDC/GDC cathodes, measured at 650°C (97% H₂ and 3% H₂O was fed to the anode while ambient air was fed to the cathode).

the composite electrodes, the BSCF/SDC electrode exhibited the lowest ASR value of 0.12 Ωcm^2 at 650°C. The BSCF itself is an excellent mixed ionic and electronic conducting material with the high ionic conductivities, even higher than SDC.²⁰⁾ However, an increase in performance can still be obtained by adding the electrolyte material with high ionic conductivity such as SDC or GDC, which can cause the enhancement of oxygen ion pathway and improvement of adhesion between cathode and electrolyte (TEC decrease).

Fig. 6 shows the electrochemical performances obtained from an anode-supported single cell with single and various composite BSCF cathodes at 650°C. In this study, Ni/YSZ anode and YSZ electrolyte were used, and GDC buffer layer was deposited on the YSZ layer in order to block the chemical reaction between Co-based cathode and YSZ

electrolyte. The cell was measured at 650°C, and the humidified hydrogen (97% H₂ and 3% H₂O) and air were fed into anode and cathode, respectively. In Fig. 6, it can be seen that the cell with BSCF cathode showed the maximum power density of 0.22 Wcm^{-2} at 650°C while the cell with BSCF/SDC and BSCF/GDC cathodes had the higher values of 0.45 Wcm^{-2} at same operating temperature. The maximum power density of single cell having a composite BSCF/SDC/GDC cathode was 0.36 Wcm^{-2} at 650°C. This trend corresponds well to the ASR value from impedance results as shown in Fig. 5.

From the results shown in Fig. 5 and 6, it can be concluded that the composite cathodes have a higher potential for IT-SOFC than single cathode. The BSCF/GDC and BSCF/SDC electrodes showed the higher electrochemical performances than that of BSCF/SDC/GDC cathode, and much higher than that of single BSCF electrode. Introducing the composite cathode could reduce the differences in TEC between cathode and electrolyte and the electrochemical performance could be improved. This can be advantages for high and stable operations of the SOFC in the intermediate ranges. However, it should be noted here that although a composite BSCF cathode and two kinds of electrolyte (BSCF/SDC/GDC) could give a positive effect in term of lowering TEC value as reported above, this composite cathode had a negative effect in term of electrochemical performance. To maximize the benefit of a composite cathode with two electrolytes, further study is required and the trade-off between TEC value and electrochemical performance should be optimized.

4. Conclusions

The characteristics and electrochemical performance of BSCF composite cathodes were investigated. Three kinds of composite cathodes were prepared and investigated (BSCF/SDC, BSCF/GDC and BSCF/SDC/GDC), compared to single BSCF cathode. As the cathode powders were mechanically mixed, three cathode composites showed their XRD patterns of perovskite and fluorite structure. The impurity phases were not detected in this study. The microstructure analysis showed that all the composite cathodes exhibited a porous structure. It was also observed from cross-sectional SEM images that the GDC and SDC powders well adhered to the cathode particles. The cathode thickness was about 20-25 μm , and the electrolyte layer was fairly dense. From the TEC measurements, it was found that the composite cathodes have lower TEC values than that of single BSCF cathode.

Among composite cathodes, the BSCF/SDC/GDC electrode showed the lowest TEC value of $18.95 \times 10^{-6} \text{ K}^{-1}$.

The composite cathodes such as BSCF/GDC and BSCF/SDC exhibited higher performance (lower ASR value) than single cathode at whole temperature ranges while the BSCF/SDC/GDC electrode showed the different electrochemical behaviors as a function of temperature. At the temperature above 600°C, the BSCF/SDC/GDC composite electrode has lower performance than single BSCF cathode. However, at lower temperature below 700°C, the electrode showed the higher performance than single BSCF cathode. Similar trend which is observed from the impedance spectra in the half cell can be observed from the IV measurements in the single cell. The anode supported single cells with BSCF/SDC and BSCG/GDC cathodes showed the maximum power densities of 0.46 Wcm^{-2} at 650°C. The cells with BSCF/SDC/GDC and single BSCF cathodes have maximum power densities of 0.36 and 0.22 Wcm^{-2} at 650°C, respectively.

By using a composite cathode (BSCF/SDC and BSCF/GDC), TEC difference between cathode and electrolyte could be reduced; and the electrochemical performance could be improved. However, when a composite BSCF cathode with two kinds of electrolyte (BSCF/SDC/GDC) was used, both positive effect of lowering TEC and negative effect of lower electrochemical performance are needed to be optimized. Further study is required to maximize the profit of using composite cathode with two electrolytes.

Acknowledgments

This research is supported by a grant from Fundamental R&D Program for Core Technology of Materials funded by the Ministry of Knowledge Economy (MKE) and this work was supported by the Brain Korea 21 (BK21) program funded by the Ministry of Education, Science Technology (MEST), Republic of Korea.

Reference

1. R.O' Hayre, S.W. Cha, W. Colella and F.B. Prinz, *Fuel Cell Fundamentals*, Wiley, New York, USA (2006).
2. S.C. Singhal and K. Kendall, *High Temperature Solid Oxide Fuel Cells*, Elsevier, Oxford, UK (2003).
3. J.H. Kim, Y. Kim, P.A. Connor and J.T.S. Irvine, J. Bae, *J. Power Sources*, **194**, 704 (2009).
4. S.P. Simmer, M.D. Anderson, J.E. Coleman and J.W. Stevenson, *J. Power Sources*, **161**, 115 (2006).
5. J.H. Kim, M. Cassidy, J.T.S. Irvine and J. Bae, *Chem. Mater.*, **22**, 883 (2010).
6. C. Fu, K. Sun, N. Zhang, X. Chen and D. Zhou, *Electrochim. Acta*, **52**, 4589 (2007).
7. Y.-M. Kim, S.-I. Pyun, J.-S. Kim and G.-J. Lee, *J. Electrochem. Soc.*, **154**, B802 (2007).
8. Y.-M. Kim and J. Bae, *ECS Transactions*, **13**, 137 (2008).
9. A. Esquirol, J. Kilner and N. Brandon, *Solid State Ionics*, **175**, 63 (2004).
10. C.R. Xia, W. Rauch, F.L. Chen and M.L. Liu, *Solid State Ionics*, **149**, 11 (2002).
11. W. Zhou, R. Ran and Z. Shao, *J. Power Sources*, **192**, 231 (2009).
12. Y.-M. Kim, P. Kim-Lohsoontorn and J. Bae, *J. Power Sources*, **195**, 6420 (2010).
13. W.-X. Kao, M.-C. Lee, T.-N. Lin, C.-H. Wang and Y.-C. Chang, *J. Power Sources*, **195**, 2220 (2010).
14. K. Wang, R. Ran, W. Zhou, H. Gu, Z. Shao and J. Ahn, *J. Power Sources*, **179**, 60 (2008).
15. O. Yamamoto, Y. Takeda, R. Kanno and M. Noda, *Solid State Ionics*, **22**, 241 (1987).
16. H.Y. Tu, Y. Takeda, N. Imanishi and O. Yamamoto, *Solid State Ionics*, **117**, 277 (1999).
17. A.M. -Amesti, A. Larrañaga, L.M.R. -Martínez, A.T. Aguayo, J.L. Pizarro, M.L. Nó, 509 A. Laresgoiti and M.I. Arriortua, *J. Power Sources*, **185**, 401 (2008).
18. Y.-M. Kim, P. Kim-Lohsoontorn, S.-W. Baek and J. Bae, *Int. J. Hydrogen Energy*, **36**, 3138 (2011).
19. S. McIntosh, J.F. Vente, W.G. Haije, D.H.A. Blank and H.J.M. Bouwmeester, *Chem. Mater.*, **18**, 2187 (2006).
20. Z.P. Shao and S.M. Haile, *Nature*, **431**, 170 (2004).